SIGMOIDAL DIAGNOSTICS WITH SOHO/CDS

G. Del Zanna[1], S.E. Gibson[1,2], H.E. Mason[1], C.D.Pike[3], and C.H. Mandrini[4]

[1]*DAMTP, University of Cambridge, Silver Street, Cambridge CB3 9EW, UK*
[2]*The Catholic University of America, Washington, DC 20064, USA*
[3]*Rutherford Appleton Laboratory, Didcot, Oxfordshire OX11 0QX, UK*
[4]*IAFE, CC67, Suc 28, 1428 Buenos Aires, Argentina*

ABSTRACT

During the third Whole Sun Month Campaign (August 18 - September 14, 1999), the evolution of the active region NOAA 8668 was followed during its meridian passage and at the limb (Sigmoid JOP 106), with simultaneous observations with the Solar and Heliospheric Observatory (SOHO), and with other instruments, both satellite and ground-based. On August 21st, a small flare, associated with a brightening of the sigmoidal structure, occurred. SOHO Coronal Diagnostic Spectrometer (CDS) observations of this small flare are presented. Coronal temperatures and densities of the sigmoid are estimated. High transition region densities (in the range 2.5-7 x 10^{11} cm^{-3}), obtained using O IV, are present in the brightenings associated with the flare. At coronal level, high temperatures of at least 8 MK were reached, as shown by strong Fe XIX emission. After this small flare, relatively strong blue-shifts ($\simeq$ 30 km/s) are observed in coronal lines, located at the two ends of a small loop system associated with the sigmoid. © 2002 COSPAR. Published by Elsevier Science Ltd. All rights reserved.

INTRODUCTION

During the third Whole Sun Month Campaign (August 18 - September 14, 1999), the evolution of the active region NOAA 8668 was followed during its meridian passage and at the limb (Sigmoid JOP 106), with simultaneous observations with SOHO and other instruments, both satellite and ground-based. This active region presented a sigmoidal, or S-shaped, structure as seen in the X-rays, had a filament associated with it for most of the time, and was very active. On August 21st, a small flare occurred (at $\simeq$ 17:40 UT). This was associated with a brightening of the sigmoidal structure as seen by e.g. YOHKOH SXT (Figure 1) and CDS.

The description of the characteristics and the evolution of this Sigmoid is the subject of various studies (e.g. Gibson et al., 2000, Ko et al., 2000). Here, we focus on the CDS observations on August 21st. The CDS data have the advantage of having spectral information, and can be used to determine plasma characteristics such as temperature, density and plasma motions (see e.g. Mason et al, 1997; Del Zanna 1999; Del Zanna and Bromage 1999a). This information can then be used in order to understand the relation between the coronal sigmoidal structure and the underlying regions, and to study the location and characteristics of the heating processes during the flare.

A large sunspot, a complex magnetic structure, and a large filament lying along the neutral line were associated with the active region during its meridian passage. On August 21st, the upper part of the filament had disappeared, while there was still a remnant of the lower part of the filament, as shown in Figure 2. This part of the filament was ejected a few hours after the small flare took place. Figure 2 also shows the presence of a small H-alpha loop system, which was very active and located in an emerging bipolar region (as seen by MDI magnetograms).

SOHO/CDS OBSERVATIONS

CDS observed the active region with the Normal Incidence Spectrometer (NIS – for more details of the CDS see e.g. Harrison et al., 1995, and Del Zanna, 1999). Due to telemetry limitations, only a limited number of NIS lines are usually extracted and telemetred to the ground. For more details of the CDS see

1999/08/21 16:13:36.652   1999/08/21 17:04:36.644   1999/08/21 17:49:24.637   1999/08/21 17:57:56.636

1999/08/21 18:06:28.635   1999/08/21 18:32:04.631   1999/08/21 19:26:28.623   1999/08/21 20:04:52.617
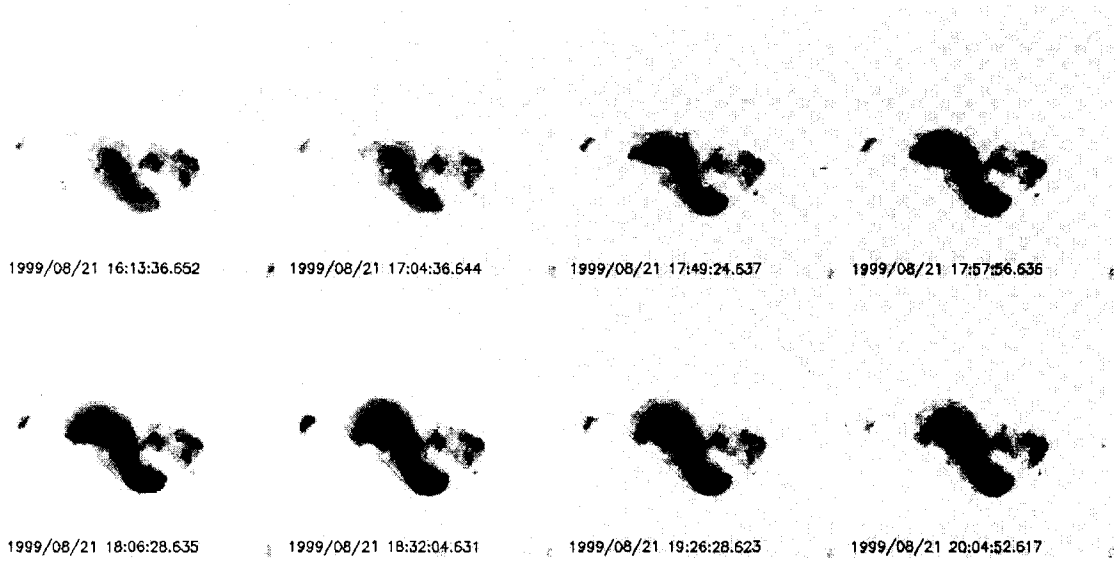
Fig. 1. YOHKOH SXT soft X-ray images. Note the presence of a small sigmoid associated with the active region. A small flare is visible in the saturated image taken at 17:49:24. Note the time evolution of the sigmoidal structure and its increasing area.

e.g. Harrison et al. (1995), and Del Zanna (1999). Two types of NIS 'studies' were used. One that takes longer (1 hour and 20 minutes) but extracts many diagnostic lines, and one faster (20 minutes), but that only extracts a few lines, selected to cover a wide range of temperatures (He I 584 Å, log T =4.5; O IV 625.9 Å, log T = 5.3; O V 630 Å, log T = 5.4; Mg X 625 Å, log T = 6.0; Si XII 520.8 Å, log T = 6.3; Fe XIX 592.2 Å, log T = 6.9). In both cases a large area ($4' \times 4'$) of the Sun was rastered with a long slit. The diagnostic study was repeated twice, once at the beginning of the observation sequence, and once at the end. In the middle, the fast raster was repeated 10 times. ' A series of standard corrections was applied to the raw NIS data. The adopted absolute intensity calibration for NIS is that one described in Del Zanna (1999). The version 2 (Landi et al., 1999) of the CHIANTI atomic database (Dere et al., 1997) has been used to calculate the line emissivities and to derive the plasma parameters.
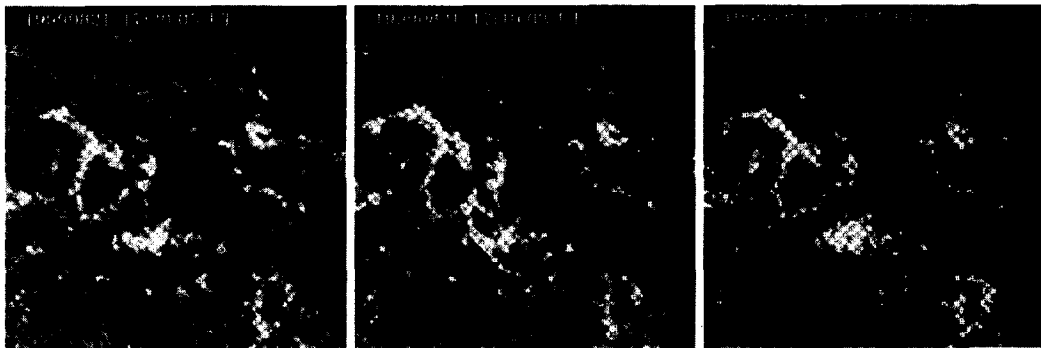
Fig. 2. Big Bear Solar Observatory (BBSO) H_α images. Note the presence of: 1) the large sunspot; 2) a remnant of the filament (compared to what was present in previous days); 3) an emerging bipolar region, just above the centre of the sigmoid, with small H-alpha loops.

The pre-flare diagnostic study

A strong brightening in the small bipolar region occurred in the high-FIP chromospheric and transition region lines (O V, Ne VI, but not in the low-FIP Mg VI). As usual, two-million degree plasma was present in the active region, as shown by Si XII and Fe XVI lines. No Fe XIX emission was present, indicating the absence of temperatures above a few million degrees. Maps of 'isothermal' temperatures (those derived from line ratios) show a sigmoidal shape. A Si XII / Mg X ratio gives temperatures in the range 1.4–1.8 x 10^6 K, while other line ratios produce different values, indicating a complex non-isothermal structure of the active region.

Line ratios from Si X show that the coronal density was 3 ± 1 x 10^9 cm^{-3}. At transition region temperatures, densities in the range 1–3 x 10^{10} cm^{-3} were derived from the O IV 625.9/554.5 Å ratio. These densities are similar to the quiet sun values reported by Del Zanna and Bromage (1999b), who studied quiet sun and coronal hole transition region densities. The transition region brightening in the small bipolar region had higher densities (6 x 10^{10} cm^{-3}). Young and Mason (1997) reported even higher densities (2 x 10^{11} cm^{-3}) in active region brightenings, also derived from O IV lines. For any physical interpretation, it should be kept in mind that these densities have the limitation of being averaged values over the line of sight. On the other hand, these measurements are direct, involving density-sensitive lines, and are independent of other parameters such as plasma filling factors.

The sigmoidal phase. The flare

Figure 3 shows the sequence of the first 4 (out of 10) monochromatic images of the CDS fast raster. The first raster shows the same structures as those of the previous diagnostic study, in particular the brightening of the small bipolar region, in the transition region lines (O V). The main difference is the presence now of a precursor small sigmoidal structure in the Fe XIX flare line.

During the second raster (centred at 17:44 UT), a small flare occurs, as seen in all lines. In the transition region (O V), the whole network structure brightens, with peak emission near the small bipolar region and the sunspot. The same applies to the coronal lines (Mg X), while in the higher-temperature lines (Si XII, Fe XIX) the peak emission is concentrated in a region in between. In particular, the flare line Fe XIX is very bright, and clearly shows where strong heating (to at least temperatures of 8 MK) takes place. During the following exposures, the emission in the hottest lines diffuses, and the sigmoid becomes more evident.

Here, we have to distinguish between the smaller sigmoidal loop system shown in the Mg X and Si XII lines (that connects to the sunspot area) and a larger sigmoidal loop system that extends out of the CDS field of view, further south-west of the sunspot, as shown by the Fe XIX intensity map. The latter is most similar to the appearance of the YOHKOH SXT images, as expected, since SXT samples high-temperature plasma. We performed linear force-free extrapolations of the photospheric magnetic field. They show the two loop systems and indicate that the brightening in the transition region lines starts in the region where the field is highly sheared and complex (where some of the field lines bend toward the northward positive pole while others are continuing on to the southward positive pole). A possible interpretation is that the magnetic field evolution may have driven the AR configuration (possibly having a twisted flux tube) to an instability. This instability, to which the emergence of the small bipolar region may have contributed, caused magnetic reconnection, creating two sets of expanding loops and a sufficient release of energy to heat the coronal plasma to at least 8MK.

Relatively strong blue-shifts ($\simeq$ 30 km/s) in the coronal lines (Mg X, Si XII) are present at the two ends of the small loop system. Figure 3 shows the Si XII velocity map (the Mg X map is very similar). For the first time, CDS has given a clear spatial indication of upflows at temperatures as low as a million degree (where Mg X is formed) starting from the onset of what was a very small flare. These upflows were located near the base of coronal loops, and can be regarded as signatures of chromospheric evaporation, following the energy release.

Zarro et al. (1988) reported the first detection of spatially-confined Mg XI blue-shifts that could be associated with chromospheric evaporation. While blue-shifts in X-ray high-temperature lines were a previously well-known phenomenon associated with flares, there was no information on their spatial location. The blue-
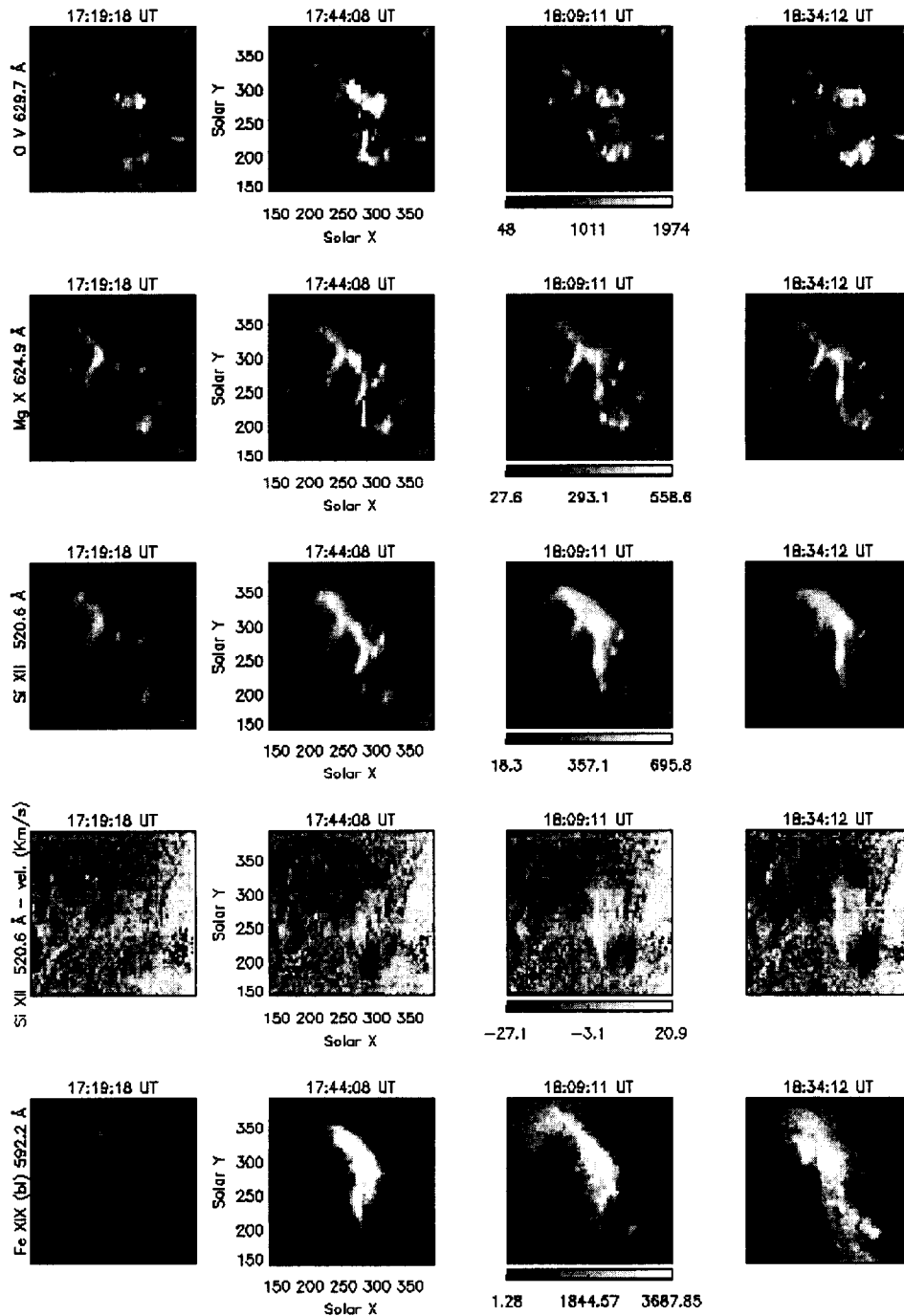
Fig. 3. A sequence of 4 CDS rasters of the Sigmoid, showing the small flare (17:44 UT). From top to bottom: monochromatic images of O V (transition region), Mg X (lower corona), Si XII (upper corona); velocity map as derived from the Si XII line profiles; monochromatic images of the Fe XIX flare line. All images in a row are plotted with the same intensity scale (shown in the third panel: phot cm^{-2} s^{-1} arcs^{-2}) for the line intensities and Km/s for the velocity map). The central time of each raster is indicated.
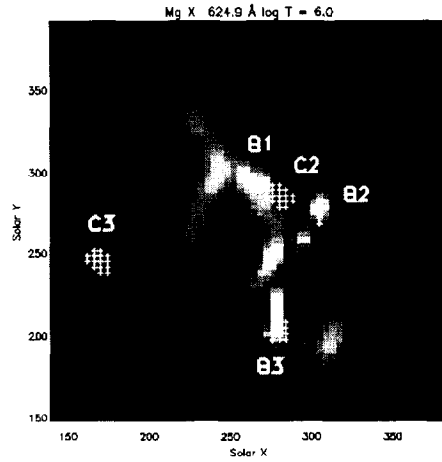
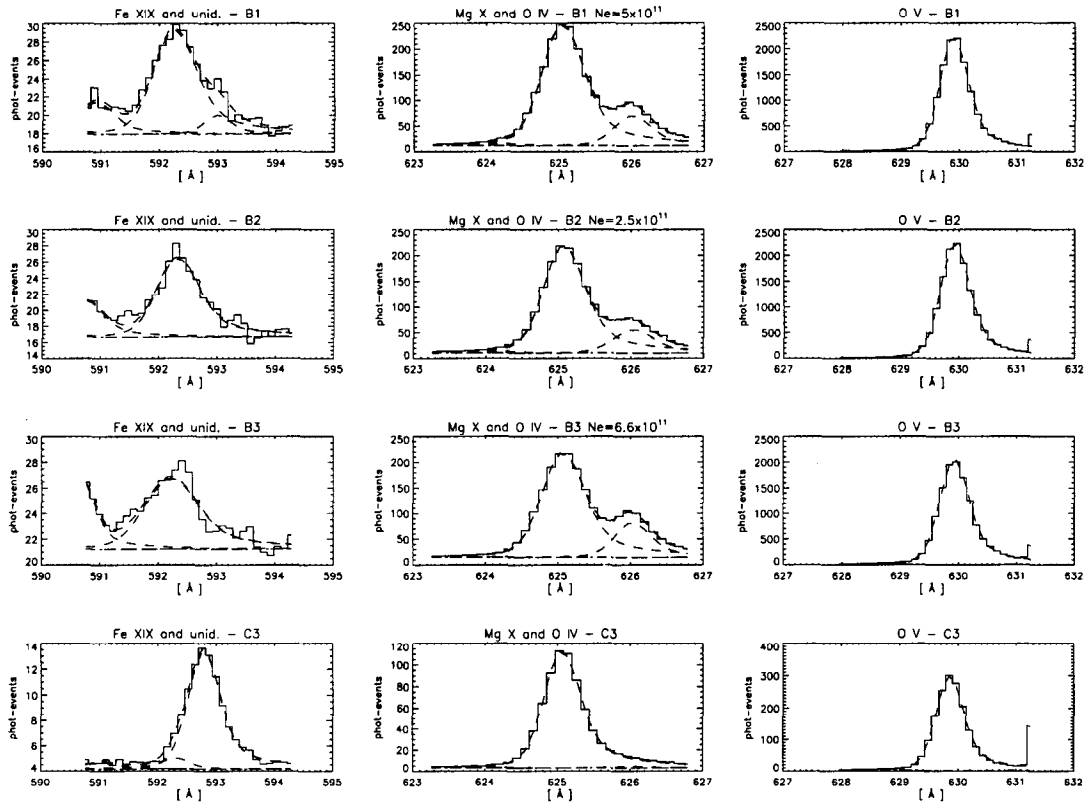Fig. 4. Selected areas, from which averaged CDS spectra were extracted.

Fig. 5. Averaged CDS spectra of a few selected regions, during the small flare. First three rows: note that in the brightenings positions (B1, B2, B3) the O IV line at 626 Å is quite intense. High densities in the range 2.5-7 $\times 10^{11}$ cm^{-3} can be derived. Last row: note that in In the C3 region, there is no Fe XIX emission. Instead, an unidentified coronal line is present. The O IV line is almost invisible, in the wing of the bright Mg X line.

shifts reported by Zarro et al. (1988) were recorded during the impulsive phase of a GOES C4 flare by the SMM Flat Crystal Spectrometer (FCS). With its collimated 14″ field of view, the FCS could only produce a limited spatial information. Recently, Czaykowska et al. (1999) also reported SOHO/CDS observations of blue-shifts in the high-temperatures Fe XVI and Fe XIX lines. The CDS observations started more than one hour after the maximum of a two-ribbon M6.8 flare, and showed some blue-shifts that appeared to be located at the outer edges of the ribbons.

In order to increase the S/N, averaged spectra were extracted from the selected areas shown in Figure 4, and line intensities calculated with a multiple broadened-gaussians line fitting (the post-recovery NIS spectra have lines with asymmetric broadened profiles). Figure 5 shows the averaged profiles of some of the spectral lines, in the three locations (B1, B2, B3) where the transition region brightenings occurred. High densities, in the range 2.5-7 x 10^{11} cm^{-3} were derived from the line ratio of the density-sensitive O IV 625.9 Å line with the O V 630 Å line, also shown in Figure 5. Strictly, this derivation assumes that no temperature effects come into play, changing the O V / O IV ratio. However, various tests on similar active region brightenings were performed, and in all cases it was found that temperature effects were negligible, i.e. the O V 630 Å / O IV 625.9 Å can be reliably used for density diagnostic. Figure 5 also shows in the last row the line profiles of the C3 area, as an example of a normal region where the emission is not due to Fe XIX 592.2 Å, but to a very close (592.6 Å) unidentified coronal line that could mistakenly be associated with Fe XIX.

During the following six CDS rasters (that lasted more than 2 hours), the blue-shifts progressively faded away, as did the Fe XIX emission. A diagnostic raster followed the series of fast rasters, and showed that in terms of densities and temperatures, the overall structure of the active region remained unchanged.

CONCLUSIONS

A small flare was observed in an active region which had a sigmoid structure. The Fe XIX emission showed some interesting properties, including a pre-flare enhancement along the sigmoid structure. Blue-shifted coronal plasma was observed at the footpoints of the Fe XIX emission, suggesting chromospheric evaporation. The electron density at transition region temperatures was found to be very high. These exciting results are part of a wider study which is in progress to understand the nature of sigmoid structures and their relationship to the magnetic field.

ACKNOWLEDGEMENTS

REFERENCES

Czaykowska, A., de Pontieu, B., Alexander, D., Rank, G, 1999, ApJ, 521, L75
Del Zanna, G. and B.J.I. Bromage, 1999a, special issue (Whole Sun Month) of JGR – Space Physics, 104, 9753.
Del Zanna, G. and B.J.I. Bromage, 1999b, ESA-SP 446, 269.
Del Zanna, G.,1999, PhD thesis, University of Central Lancashire, UK.
Dere, K.P., Landi, E., Mason, H.E., Monsignori Fossi, B.C. and Young, P.R.,1997, A&ASS 125, 149.
Gibson, S., et al., 2000, IAU203, E.105G.
Harrison, R.A., et al., 1995, Sol. Phys., 162, 233.
Ko, Y.-K., et al., 2000, AAS-SPD 32, 2.71.
Landi, E., Landini, M., Dere, K.P., Young, P.R.. and Mason, H. E., 1999, A&A, 135, 339.
Mason H.E., Young P.R., Pike C.D., Harrison R.A., Fludra A., Bromage B.J.I., Del Zanna G., 1997, Sol. Phys., 170, 143.
Young, P.R. and Mason H.E., 1997, Sol. Phys., 175,523.
Zarro, D.M., Slater, G.L., and Freeland, S.L., 1988, ApJ, 333, L99.